ELSEVIER

Journal of Nuclear Materials 250 (1997) 192–199

journal of nuclear materials

A swelling model for stoichiometric SiC at temperatures below 1000°C under neutron irradiation

Hanchen Huang [a], Nasr Ghoniem [b,*]

[a] *Lawrence Livermore National Laboratories, P.O. Box 808, L-268, Livermore, CA 94550, USA*

[b] *Mechanical and Aerospace Engineering Department, School of Engineering and Applied Science, University of California Los Angeles, Box 95197, 420 Westwood Plaza, Los Angeles, CA 90095-1600, USA*

Received 2 January 1996; accepted 24 July 1997

Abstract

A simple phenomenological model for the saturation swelling below 1000°C of neutron-irradiated silicon carbide (SiC) is presented in this paper. Under fast neutron irradiation, SiC is known to undergo volumetric expansion (swelling) which quickly saturates at a fast fluence of approximately 10^{25} n/m^2 for irradiation temperatures below 1000°C. A previous model due to Balarin attributes swelling to lattice dilation as a result of single point defects. We show in this paper that the experimentally observed linear temperature dependence of saturation swelling can be explained in terms of the formation and growth of small interstitial clusters, resulting directly from collision cascades initiated by energetic neutrons. These loops grow by absorption of mobile carbon interstitials and their composition is subject to stoichiometry constraints, requiring absorption of slower silicon interstitials. Because of cascade re-solution events, the density of loops decreases sharply with temperature as a result of overlap of cascades with larger size loops at higher temperatures. The average radius of these loops increases with temperature. Volumetric swelling is shown to obey a linear temperature dependence as a consequence of the strong decrease in density and the simultaneous increase in average radius, and to saturate with fluence. The model is shown to be consistent with experimental observations. In the temperature range below 500–600°C, swelling seems to be dominated by single point defects, or defect clusters containing only a few atoms, in accordance with the explanation offered by Balarin. © 1997 Elsevier Science B.V.

1. Introduction

The dimensional stability of neutron-irradiated silicon carbide (SiC) is a key issue in its utilization in any nuclear environment. Several applications of SiC in the nuclear industry have prompted investigation of its dimensional stability, as far back as the early 1950s [1]. Other applications for SiC include its utilization in high temperature monitors in nuclear reactors [2–4] and as a coating material for high temperature gas-cooled reactor (HTGR) fuel elements [5–12]. Recent interest in SiC has been motivated by its possible utilization as a structural material in fusion energy system [13,14]. Because of its low activation characteristics, its dimensional stability under neutron irradiation becomes even more important as a structural material in fusion energy systems. More recent investigations on the effects of neutron irradiation are given in Refs. [15–24] [25–29] and the experimental swelling data are well presented by Price and co-workers [7,9,30] and by Blackstone and Voice [8].

The main objective of the present work is to critically examine available experimental data on neutron induced swelling and to present a phenomenological model which is consistent with this data. The possibility of this re-examination is a result of a number of considerations, as listed below.

(1) New experimental data on the swelling behavior of neutron irradiated SiC have become more available because of the interest in applications of SiC/SiC composites in fusion energy systems.

(2) The Balarin model [31] does not lend itself to an

* Corresponding author. Fax: +1-310 206 4830.

PII S0022-3115(97)00269-9

explanation of the linear temperature dependence of volumetric swelling below 1000°C. We emphasize in this paper the contribution to swelling from point defect clusters, as contrasted to single point defects in the Balarin model.

(3) Our recent work on molecular dynamics (MD) simulations for the energetics of point defects in β-SiC crystals [32,33] can now provide critical information on the migration and formation energies of point defects. Thus, deeper physical insight can be gained in considering the behavior of atomic defects in β-SiC.

Experimental investigations of the swelling behavior of SiC have mainly considered two polytypes: 6H and 3C (or β type). At temperatures below 1000°C, it has been found that the two polytypes undergo volumetric expansion in a similar fashion, when irradiated by neutrons. The dilatation in volume is found to be isotropic in both cases. The

Table 1

Temperature (°C)	Swelling (%) (lattice expansion)	Sample	Fluence (spectrum) (n/cm^2)	Facility	Ref.
(1) Saturation swelling data base for stoichiometric SiC					
120	(1.03, 1.03)	α-SiC	7.2e24 (unspecified)	RFT	Pravdyuk, 1962 [2]
180	(0.73, 0.73)	α-SiC	7.2e24 (unspecified)	RFT	Pravdyuk, 1962 [2]
370	0.44 (0.50)	RB-β-SiC	1.5e26 ($E > 0.1$ MeV)	JOYO, Phenix, Rapsodie	Miyazaki, 1992 [17]
420	(0.58, 0.58)	α-SiC	7.2e24 (unspecified)	RFT	Pravdyuk, 1962 [2]
425	(0.52, 0.52)	α-SiC	1.3e25 ($E > 0.18$ MeV)	WR-1	Stevens, 1972 [11]
460	0.36 (0.34)	Py-β-SiC	2.7e25 ($E > 0.18$ MeV)	unspecified	Price, 1977 [30]
460	0.36 (0.34)	Py-β-SiC	2.7e25 ($E > 0.18$ MeV)	ETR	Price, 1969 [7]
470	0.45 (0.46)	RB-β-SiC	3.0e24 ($E > 0.1$ MeV)	JOYO, Phenix, Rapsodie	Miyazaki, 1992 [17]
480	0.28	RB-β-SiC	1.7e27 ($E > 0.1$ MeV)	JOYO, Phenix, Rapsodie	Miyazaki, 1992 [17]
525	0.50	HP-α-SiC	4.8e25 ($E > 0.18$ MeV)	ETR	Price, 1972 [5]
460–610	0.27 (0.12)	Py-β-SiC	9.7e25 ($E > 0.18$ MeV)	unspecified	Price, 1977 [30]
550	0.35	β-SiC	2.6–3.4e24 (fast)	PLUTO	Palentine, 1976 [4]
620	0.23 (0.11)	RB-β-SiC	4.8e26 ($E > 0.1$ MeV)	JOYO, Phenix, Rapsodie	Miyazaki, 1992 [17]
620	0.23 (0.19)	Py-β-SiC	2.7e25 ($E > 0.18$ MeV)	ETR	Price, 1969 [7]
630	0.24 (0.20)	Py-β-SiC	2.8e25 ($E > 0.18$ MeV)	ETR	Price, 1969 [7]
650	0.29	β-SiC	3.6–4.1e24 (fast)	PLUTO	Palentine, 1976 [4]
700	0.30 (0.33)	Py-β-SiC	3.8e25 ($E > 0.18$ MeV)	ETR	Price, 1969 [7]
750	0.22	β-SiC	3.6–4.1e24 (fast)	PLUTO	Palentine, 1976 [4]
772	0.30	HP-α-SiC	4.8e25 ($E > 0.18$ MeV)	ETR	Price, 1972 [5]
950–1040	0.14 (0.03)	Py-β-SiC	12.2e25 ($E > 0.18$ MeV)	unspecified	Price, 1977 [30]
980	0.07 (0.07)	Py-β-SiC	4.2e25 ($E > 0.18$ MeV)	ETR	Price, 1969 [7]
1010	0.03 (0.05)	Py-β-SiC	2.0e25 ($E > 0.18$ MeV)	ETR	Price, 1969 [7]
1010	0.06 (0.05)	Py-β-SiC	2.7e25 ($E > 0.18$ MeV)	ETR	Price, 1969 [7]
1020	0.08 (0.03)	Py-β-SiC	2.8e25 ($E > 0.18$ MeV)	ETR	Price, 1969 [7]
1040	0.06 (0.10)	Py-β-SiC	3.8e25 ($E > 0.18$ MeV)	ETR	Price, 1969 [7]
1040	0.10 (0.10)	Py-β-SiC	3.8e25 ($E > 0.18$ MeV)	unspecified	Price, 1977 [30]
(2) Non-saturated or non-stoichiometric swelling data of SiC					
30	1.24	α-SiC	3.0e24 (unspecified)	MTR and EBR	Primak, 1956 [1]
120	0.90	α-SiC	saturation	unspecified	Balarin, 1965 [31]
140	0.40	B^{10} + RB-SiC	3.6e24 ($E > 1$ MeV)	HFBR	Corelli, 1982 [19]
140	2.40	B^{10} + RB-SiC	7.6e24 ($E > 1$ MeV)	HFBR	Corelli, 1982 [19]
140	0.28	B^{11} + RB-SiC	3.6e24 ($E > 1$ MeV)	HFBR	Corelli, 1982 [19]
140	0.40	B^{11} + RB-SiC	7.6e24 ($E > 1$ MeV)	HFBR	Corelli, 1982 [19]
140	0.10	B + RB-SiC	3.6e24 ($E > 1$ MeV)	HFBR	Corelli, 1982 [19]
140	0.47	B + RB-SiC	7.6e24 ($E > 1$ MeV)	HFBR	Corelli, 1982 [19]
140	0.47	B^{10} + α-SiC	3.6e24 ($E > 1$ MeV)	HFBR	Corelli, 1982 [19]
140	0.63	B^{10} + α-SiC	7.6e24 ($E > 1$ MeV)	HFBR	Corelli, 1982 [19]
140	0.53	B^{11} + α-SiC	3.6e24 ($E > 1$ MeV)	HFBR	Corelli, 1982 [19]
140	0350	B^{11} + α-SiC	7.6e24 ($E > 1$ MeV)	HFBR	Corelli, 1982 [19]
140	0.63	B + α-SiC	3.6e24 ($E > 1$ MeV)	HFBR	Corelli, 1982 [19]
140	0.34	B + α-SiC	7.6e24 ($E > 1$ MeV)	HFBR	Corelli, 1982 [19]

Table 1 (continued)

Temperature (°C)	Swelling (%) (lattice expansion)	Sample	Fluence (spectrum) (n/cm^2)	Facility	Ref.
200	0.83	α-SiC	saturation	unspecified	Balarin, 1965 [34]
250	0.80 (0.70)	SB-β-SiC	4.7e24 (fast)	DMTR	Thorne, 1967 [6]
250	0.76 (0.76)	SB-β-SiC	5.5e24 (fast)	DMTR	Thorne, 1967 [6]
250	0.82 (0.72)	SB-β-SiC	1.1e25 (fast)	DMTR	Thorne, 1967 [6]
250	0.69 (0.67)	SB-β-SiC	1.4e25 (fast)	DMTR	Thorne, 1967 [6]
250	0.68 (0.65)	SB-β-SiC	1.7e25 (fast)	DMTR	Thorne, 1967 [6]
270	0.84 (0.73, 0.77)	α-SiC	2.5e25 (unspecified)	MTR and EBR	Primak, 1956 [1]
270	0.88 (0.89, 1.09)	α-SiC	1.1e25 (unspecified)	MTR and EBR	Primak, 1956 [1]
300	0.74	α-SiC	saturation	unspecified	Balarin, 1965 [31]
400	0.64	α-SiC	saturation	unspecified	Balarin, 1965 [31]
450	(0.11, 0.27)	α-SiC	3.2e24 ($E > 1$ MeV)	unspecified	Mathews, 1974 [12]
450	(0.29, 0.39)	α-SiC	6.0e24 ($E > 1$ MeV)	unspecified	Mathews, 1974 [12]
450	(0.39, 0.38)	α-SiC	1.0e25 ($E > 1$ MeV)	unspecified	Mathews, 1974 [12]
450	(0.29, 0.35)	α-SiC	3.0e25 ($E > 1$ MeV)	unspecified	Mathews, 1974 [12]
450	0.48	β-SiC	3.6–4.1e24 (fast)	PLUTO	Palentine, 1976 [12]
475	0.43 (0.45)	SB-β-SiC	4.5e24 (fast)	DMTR	Thorne, 1967 [6]
475	0.43 (0.45)	SB-β-SiC	5.0e24 (fast)	DMTR	Thorne, 1967 [6]
475	0.40 (0.42)	SB-β-SiC	1.0e25 (fast)	DMTR	Thorne, 1967 [6]
475	0.47 (0.48)	SB-β-SiC	1.0e25 (fast)	DMTR	Thorne, 1967 [6]
475	0.42 (0.42)	SB-β-SiC	1.8e25 (fast)	DMTR	Thorne, 1967 [6]
480	0.31	Py-β-SiC	4.8e24 ($E > 0.18$ MeV)	HFR and HFIR	Blackstone, 1971 [8]
480	0.30	SB-β-SiC	4.8e25 ($E > 0.18$ MeV)	HFR and HFIR	Blackstone, 1971 [8]
510	0.55	α-SiC	saturation	unspecified	Balarin, 1965 [31]
560	0.32	SB-β-SiC	3.0e24 ($E > 0.18$ MeV)	HFR and HFIR	Blackstone, 1971 [8]
600	0.36	Py-β-SiC	5.0e25 ($E > 0.18$ MeV)	HFR and HFIR	Blackstone, 1971 [8]
600	0.48	α-SiC	saturation	unspecified	Balarin, 1965 [31]
600	0.38	SB-β-SiC	2.2e25 ($E > 0.18$ MeV)	HFR and HFIR	Blackstone, 1971 [8]
600	0.35	SB-β-SiC	2.7e25 ($E > 0.18$ MeV)	HFR and HFIR	Blackstone, 1971 [8]
600	0.28	Si + SiC	4.3e24 ($E > 1$ MeV)	JMTR	Suzuki, 1990 [27]
600	0.35	B + C + SiC	4.3e24 ($E > 1$ MeV)	JMTR	Suzuki, 1990 [27]
600	0.39	BeO + SiC	4.3e24 ($E > 1$ MeV)	JMTR	Suzuki, 1990 [27]
625	0.19	Py-β-SiC	6.0e24 ($E > 0.18$ MeV)	ETR	Price, 1973 [9]
625	0.19	Py-β-SiC	9.0e24 ($E > 0.18$ MeV)	ETR	Price, 1973 [9]
640	0.22	Si + SiC	6.0e24 ($E > 1$ MeV)	JMTR	Suzuki, 1990 [27]
640	0.32	B + C + SiC	6.0e24 ($E > 1$ MeV)	JMTR	Suzuki, 1990 [27]
640	0.31	BeO + SiC	6.0e24 ($E > 1$ MeV)	JMTR	Suzuki, 1990 [27]
650	(0.24, 0.36)	α-siC	3.2e24 ($E > 1$ MeV)	unspecified	Mathews, 1974 [12]
650	(0.39, 0.49)	α-siC	6.0e24 ($E > 1$ MeV)	unspecified	Mathews, 1974 [12]
650	(0.32, 0.36)	α-siC	3.0e25 ($E > 1$ MeV)	unspecified	Mathews, 1974 [12]

swelling of SiC under neutron irradiation increases with the irradiation dose, and reaches saturation levels at a fast neutron fluence of approximately 10^{25} n/cm^2 at temperatures below 1000°C. At temperatures above approximately 1000°C, neutron induced volumetric swelling does not saturate with fluence. In addition, the temperature dependence of swelling is not linear above 1000°C. The swelling mechanisms are therefore of different origins for temperatures below and above 1000°C. We will confine our attention here to the mechanism of swelling below 1000°C.

Because of the poor understanding of basic point defect energetics in SiC, comprehensive modeling of neutron irradiation induced swelling has been lacking. With recent MD investigations of the nature and energetics of point defects in SiC [32,33], it is now possible to shed some light on radiation induced swelling mechanism in SiC. Available irradiation swelling data is discussed in Section 2, with the intent of critically assessing valid data for our model. In Section 3, we discuss the previous model of Balarin and develop a new phenomenological description

Table 1 (continued)

Temperature (°C)	Swelling (%) (lattice expansion)	Sample	Fluence (spectrum) (n/cm^2)	Facility	Ref.
700	0.32 (0.27)	SB-β-SiC	3.5e24 (fast)	DMTR	Thorne, 1967 [6]
700	0.29 (0.24)	SB-β-SiC	6.5e24 (fast)	DMTR	Thorne, 1967 [6]
700	0.28 (0.31)	SB-β-SiC	6.5e24 (fast)	DMTR	Thorne, 1967 [6]
700	0.32 (0.33)	SB-β-SiC	8.0e24 (fast)	DMTR	Thorne, 1967 [6]
700	0.37 (0.31)	SB-β-SiC	1.8e25 (fast)	DMTR	Thorne, 1967 [6]
700	0.33 (0.33)	SB-β-SiC	1.8e25 (fast)	DMTR	Thorne, 1967 [6]
800	0.15	Py-β-SiC	5.4e25 ($E > 0.18$ MeV)	HFR and HFIR	Blackstone, 1971 [8]
900	0.19	SB-β-SiC	3.0e25 ($E > 0.18$ MeV)	HFR and HFIR	Blackstone, 1971 [8]
900	0.14	SB-β-SiC	3.1e25 ($E > 0.18$ MeV)	HFR and HFIR	Blackstone, 1971 [8]
900	0.20	SB-β-SiC	4.5e25 ($E > 0.18$ MeV)	HFR and HFIR	Blackstone, 1971 [8]
900	0.19	SB-β-SiC	4.6e25 ($E > 0.18$ MeV)	HFR and HFIR	Blackstone, 1971 [8]
900	0.15	SB-β-SiC	2.0e25 ($E > 0.18$ MeV)	HFR and HFIR	Blackstone, 1971 [8]
900	0.14	SB-β-SiC	2.1e25 ($E > 0.18$ MeV)	HFR and HFIR	Blackstone, 1971 [8]
900	0.11	SB-β-SiC	8.5e24 ($E > 0.18$ MeV)	HFR and HFIR	Blackstone, 1971 [8]
900	0.10	SB-β-SiC	8.6e24 ($E > 0.18$ MeV)	HFR and HFIR	Blackstone, 1971 [8]
900	0.105	SB-β-SiC	5.0e24 ($E > 0.18$ MeV)	HFR and HFIR	Blackstone, 1971 [8]
900	0.095	SB-β-SiC	4.8e25 ($E > 0.18$ MeV)	HFR and HFIR	Blackstone, 1971 [8]
900	0.03	SB-β-SiC	1.4e25 ($E > 0.18$ MeV)	ETR	Price, 1973 [9]
900	0.03	SB-β-SiC	2.4e25 ($E > 0.18$ MeV)	ETR	Price, 1973 [9]
1000	0.14	Py-B-SiC	12.4e25 ($E > 0.18$ MeV)	ETR	Price, 1973 [9]
1050	0.06	Py-B-SiC	3.8e25 ($E > 0.18$ MeV)	ETR	Price, 1973 [9]
1200	0.04	SB-β-SiC	3.5e24 ($E > 0.18$ MeV)	HFR and HFIR	Blackstone, 1971 [8]
1200	0.06	SB-β-SiC	5.0e24 ($E > 0.18$ MeV)	HFR and HFIR	Blackstone, 1971 [8]
1200	0.05	SB-β-SiC	6.0e24 ($E > 0.18$ MeV)	HFR and HFIR	Blackstone, 1971 [8]
1200	0.10	SB-β-SiC	6.5e24 ($E > 0.18$ MeV)	HFR and HFIR	Blackstone, 1971 [8]
1200	0.10	Py-β-SiC	9.5e24 ($E > 0.18$ MeV)	HFR and HFIR	Blackstone, 1971 [8]
1200	0.19	SB-β-SiC	1.4e25 ($E > 0.18$ MeV)	HFR and HFIR	Blackstone, 1971 [8]
1200	0.21	SB-β-SiC	1.6e25 ($E > 0.18$ MeV)	HFR and HFIR	Blackstone, 1971 [8]
1200	0.25	SB-β-SiC	2.1e25 ($E > 0.18$ MeV)	HFR and HFIR	Blackstone, 1971 [8]
1200	0.24	Py-β-SiC	2.2e25 ($E > 0.18$ MeV)	HFR and HFIR	Blackstone, 1971 [8]
1200	0.29	SB-β-SiC	2.5e25 ($E > 0.18$ MeV)	HFR and HFIR	Blackstone, 1971 [8]
1200	0.28	SB-β-SiC	2.9e25 ($E > 0.18$ MeV)	HFR and HFIR	Blackstone, 1971 [8]
1200	0.35	SB-β-SiC	3.3e25 ($E > 0.18$ MeV)	HFR and HFIR	Blackstone, 1971 [8]
1200	0.38	Py-β-SiC	3.6e25 ($E > 0.18$ MeV)	HFR and HFIR	Blackstone, 1971 [8]
1200	0.39	SB-β-SiC	4.2e25 ($E > 0.18$ MeV)	HFR and HFIR	Blackstone, 1971 [8]
1250	0.27	Py-β-SiC	4.3e25 ($E > 0.18$ MeV)	ETR	Price, 1973 [9]
1275	0.43	Py-β-Sic	7.4e25 ($E > 0.18$ MeV)	ETR	Price, 1973 [9]
1500	0.30	Py-β-SiC	5.2e25 ($E > 0.18$ MeV)	ETR	Price, 1973 [9]
1500	0.37	Py-β-Sic	8.8e25 ($E > 0.18$ MeV)	ETR	Price, 1973 [9]

of irradiation swelling in β-SiC. Discussions and conclusions are finally given in Section 4.

2. Experimental swelling data: An assessment

Experimental investigations on the swelling of SiC irradiated by energetic neutrons spanned several decades. On a number of occasions, available data has been reviewed [7–9,30]. Since more swelling data has become available, it is now desirable to summarize it. Our intent is to assess the applicability of the proposed model to the existing data base. In Table 1, we list available data for neutron induced swelling of SiC and the special experimental conditions for each data point. The data is grouped into two categories: (1) data for stoichiometric, pure SiC with saturation fluence and (2) data for doped SiC, crusilites, or any SiC irradiated with low neutron fluence.

The neutron spectrum in Ref. [1] was not specified with a fluence of 3×10^{24} n/cm^2. It is possible that saturation had not been reached in this experiment. This data is therefore placed in Table 1(2). Reaction bonded SiC was used in Ref. [12] with a large percentage of free silicon which was present at grain boundary. The swelling in these samples was found to be dominated by this phase initially which gives rise to initial contraction, followed by nearly

isotropic expansion. Since it is not clear how much the free silicon contributes to the total swelling, this set of data is also classified in Table 1(2). Due to the same reason, data from Ref. [27] is left in Table 1(2). Swelling data in Ref. [19] is not used in Table 1(1) because of boron impurity atoms which has a large (n, α) reaction cross-section. The α-particles (helium atoms) stabilize vacancy clusters and can have a dramatic impact on over all swelling behavior. The experimental data quoted by Balarin is excluded in Table 1(1) because of low neutron fluence in the experiment. In Ref. [11], swelling data for several values of the neutron fluence are given. We include only the data with highest neutron fluence in Table 1(1) for saturation swelling. In Refs. [6,8], crusilites are used. They are very low density SiC and most likely have free silicon atoms at grain boundaries. These data are therefore excluded from Table 1(1) as well. Although the spectrum in Ref. [2] was not specified, the data is considered to correspond to saturation swelling because of the higher fluence and is therefore included in Table 1(1). The macroscopic linear swelling and lattice expansion results are listed in the same column, with parentheses indicating lattice expansion. For lattice expansion of 6H SiC, values along basal and vertical directions are also gioven.

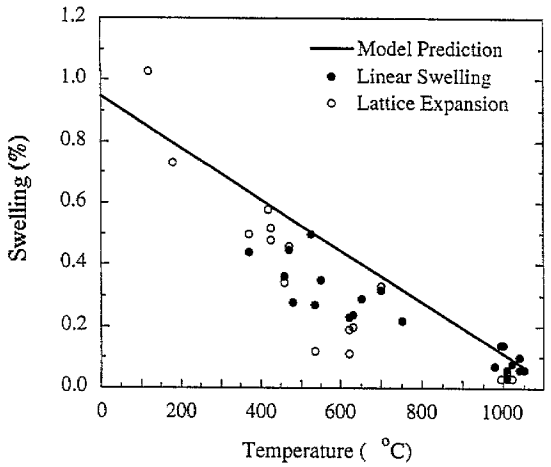

Fig. 1. Comparison of experimental linear swelling data (solid circles) and lattice expansion (open circles) with our model predictions (solid line).

3. Phenomenological model

The phenomenological model described in this section is based on a number of assumptions which will be outlined here. However, we wish to give a brief summary of a previous model for swelling in SiC proposed by Balarin [31]. In the Balarin model, the rate of change of Frenkel pair concentration (N) is assumed to be proportional to the neutron flux (Φ) and the yield of Frenkel pairs per neutron (A). The time evolution equation, as given by Balarin, is therefore

$$\frac{dN}{dt} = \Phi_A(1 - 2\alpha N), \tag{1}$$

where α is the recombination volume per defect. The parameters α and A are actually fitted to macroscopic experimental swelling data available at the time, in the range of 200–500°C. For saturation fluence, Balarin developed an empirical fit to the parameter α by noting that the saturation swelling of Frenkel pairs is given by

$$N|_{t\to\infty} = \frac{1}{2\alpha}. \tag{2}$$

Balarin's fit produced the following value for α (and hence $N|_{t\to\infty}$):

$$\frac{d\ln\alpha}{dt} = -\frac{d\ln N_\infty}{dt} = 1.2\times10^{-3}\,°C^{-1}. \tag{3}$$

The experimental temperature dependence of swelling is clear from the above equation, if the volume per defect is not sensitive to temperature. However, in the small range of temperatures investigated by Balarin, the above equation produces a near-linear dependence on temperature for the macroscopic swelling.

We propose here a model which departs from that of Balarin in a number of areas. First, we consider swelling to result from clustering of carbon interstitial atoms produced directly from cascades. Silicon defects are much slower and hence the rate of swelling is primarily controlled by the clustering rate of silicon interstitials. Second, we assume that stoichiometric interstitial loops grow by absorption of single defects and shrink due to line tension effects and hence the growth rate is expected to be sensitive to temperature. Third, Balarin concluded that the effective migration energy for defects is in the range of 0.01–0.03 eV in SiC, although it is not clear how this value was used in his analysis of saturation swelling. Our recent MD calculations [32,33] indicate that the smallest migration energy for point defects is 1.3 eV in SiC, which is in sharp contrast with his conclusions. In addition, the experimental

Table 2
Physical parameters used in the model

Parameter	Numerical value	Unit	Ref.
μ	1110	eV/nm^3	[35]
ν	0.17	none	[36]
ε_i	0.3	none	estimated
γ_{sf}	1.56×10^{-2}	eV/nm^2	[37]
E_i^f	3.5	eV	[33]
E_i^m	1.3	eV	[33]
E_s	2.8	eV	estimated
K_i	1.0×10^{-6}	nm^{-2}	estimated
P_i	1.0×10^{-6}	eV	[38]
α	25	none	estimated

data base we assembled in this work is substantially larger than that used by Balarin and covers a much wider temperature range (100–1000°C).

According to our recent MD simulations with the modified EAM potential [33], migration energies of a silicon vacancy, a silicon interstitial, a carbon vacancy and a carbon interstitial are 2.7, 4.1, 2.6 and 1.3 eV, respectively. Therefore, carbon interstitials are mobile, even at room temperature, while vacancies and silicon interstitials are immobile below 1000°C. Pre-exponential factors of point defect diffusion coefficients are close to 10^{-7} m^2/s and are taken to be equal for all point defects.

Vacancies can be produced either in single point defects or in clusters (loops at low temperatures). In the simple phenomenological model presented here, we assume that vacancy clusters surviving from cascades will soon be destroyed by self-interstitials. This is consistent with recent experimental observations that dislocation loops are mainly of the interstitial type [34]. Therefore, vacancy loops do not contribute to low temperature swelling directly, and will be described as a background sink for mobile defects. Our MD calculations show that vacancies can hardly migrate and will therefore be considered as another background sink for mobile defects. Silicon interstitials play a different role in the sense that they form interstitial loops with carbon interstitials. They determine growth/shrinkage of interstitial loops through stoichiometry requirements, which is unique for multi-component systems. The species that are actively evolving are carbon interstitials and interstitial loops. The interstitial loops grow by absorbing carbon interstitials subject to stoichiometry requirements and they shrink by thermal emission of carbon interstitials. Thermal emission of silicon interstitials is omitted due to their extremely large formation energies. The density of interstitial loops is determined by a competition between production from cascades and destruction by overlapping with other cascades. Based on the above assumptions and the conventional adiabatic assumption for fast species (i.e. point defects), the governing equations for carbon interstitials and interstitial loops are given as

$$\varepsilon_i P + D_i C_i^e e^{(\gamma_{sf}+F_{el})b^2/kT}(2\pi rn) = D_i C_i K_i + e^{-E_s/kT} D_i C_i (2\pi rn), \tag{4}$$

$$\frac{dr}{dt} = \frac{1}{b}\left[D_i C_i e^{-E_s/kT} - D_i C_i^e e^{(\gamma_{sf}+F_{el})b^2/kT} \right], \tag{5}$$

with

$$F_{el} = \frac{\mu b^2}{(1-\nu)4\pi r}, \tag{6}$$

$$\frac{dn}{dt} = P_n - \alpha P_n n\left(\frac{4}{3}\pi r^3\right). \tag{7}$$

The bias factor of dislocation loops toward interstitials is taken as unity, since no vacancy is considered. E_s is defined as the difference between the migration energies of silicon and carbon interstitials and is introduced to represent the tendency of interstitial loops toward stoichiometry. D_i is the diffusivity of carbon interstitials, K_i represents the strength of background sinks, r and n are average radius and volume density of the interstitial loops, respectively, γ_{sf} is the stacking fault energy, μ is the shear modulus, ν is Poisson's ratio, b is Burgers vector and, finally, α is an effective cascade resolution efficiency. Eq. (4) represents the steady state balance of carbon interstitials, while Eqs. (5) and (7) are for the rates of change of the average loop radius and number density, respectively.

At steady-state (i.e. saturation swelling conditions), both r and n are time independent. Eqs. (5) and (7) take the form

$$D_i C_i e^{-E_s/kT} = D_i C_i^e e^{(\gamma_{sf}+F_{el})b^2/kT}, \tag{8}$$

$$\alpha n\left(\frac{4}{3}\pi r^3\right) = 1. \tag{9}$$

Combining Eqs. (4), (8) and (9), we have

$$r = \frac{\mu b^4}{4\pi(1-\nu)} \times \frac{1}{E_i^f - E_s - \gamma_{sf}b^2 + E_i^m - kT\ln\left(K_i D_i^0/\varepsilon_i P\right)} = \frac{1}{\chi - \psi T}, \tag{10}$$

where

$$\chi = \frac{4\pi(1-\nu)}{\mu b^4}\left(E_i^f - E_s - \gamma_{sf}b^2 + E_i^m\right), \tag{11}$$

$$\psi = \frac{4\pi(1-\nu)}{\mu b^4} k\ln\left(K_i D_i^0/\varepsilon_i P\right), \tag{12}$$

where the thermal emission rate is assumed to be much smaller than the production rate of carbon interstitials from cascades. Interstitial loops are much weaker than background sinks to attract interstitials due to stoichiometry constraints. With a set of typical parameters listed in Table 2, we have

$$r = \frac{1}{0.468 - 3.329\times10^{-4}T\ (\mathrm{K})}\ (\text{Å}). \tag{13}$$

Using Eq. (9), we obtain the linear swelling

$$\frac{\Delta L}{L} = \frac{1}{3}n\pi r^2 b = \frac{1}{\alpha}\left(0.294 - 2.095\times10^{-4}T\ (\mathrm{K})\right). \tag{14}$$

With an effective cascade resolution efficiency, α, taken as 25, the predicted saturated swelling is compared with experimental swelling data in Fig. 1. The temperature dependence of the average radius, r, is shown in Fig. 2,

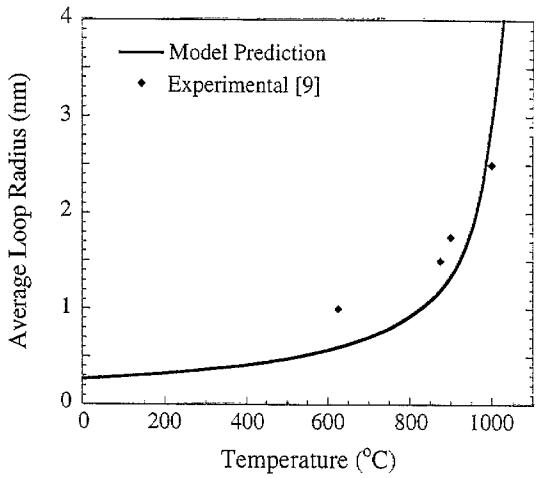

Fig. 2. Comparison of average loop radius predicted by our model (solid line) with experimental measurements (solid diamonds).

where measurements by Price [9] are compared with our model prediction in Fig. 2. The contribution of swelling from single carbon interstitials is negligible. This can be seen by considering the concentration of single carbon interstitials, using the parameters presented in Table 2. It can be shown that the swelling caused by carbon interstitials is less than 0.01%, which is small compared with that due to the contribution of interstitial loops Since lattice dilation measurements are on the same order as the macroscopic swelling, at least up to 700°C, the swelling caused by interstitial loops is also manifest in free vacancies in this lower temperature range. However, above 700°C, it appears that the size of interstitial loops is large and that vacancies may be forming clusters as well, thus separating lattice dilation measurements from volumetric swelling, as can be observed from Fig. 3.

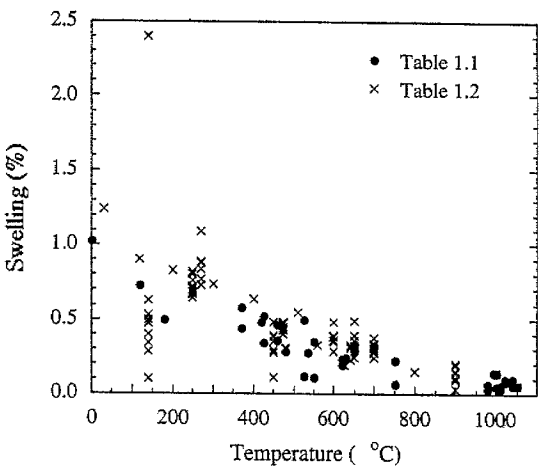

Fig. 3. Comparison of data listed in Table 1(1) (solid circles) and (2) (crosses).

4. Discussion and conclusions

The phenomenological model presented in this paper seems to be consistent with the majority of experimental data on the volumetric swelling and lattice dilatation of pure, stoichiometric SiC. One important aspect of this model is that it reproduces the linear temperature dependence of saturation swelling of neutron-irradiated SiC. The model is based on the formation of small interstitial loops in cascades and their subsequent growth by the absorption of the only mobile species in the temperature range below 1000°C: carbon interstitials. This is contrasted with an earlier model by Balarin, where single point defects are assumed to contribute to swelling. It is argued that the contribution to swelling from single point defects does not result in a linear dependence on temperature and that it may be valid for very low temperatures, below 700°C. The following specific conclusions can be drawn from the present model.

(1) For purposes of comparison with the present model, the data of Corelli et al. [19], Matthews [12] and Suzuki et al. [27] are excluded because of the presence of free silicon in reaction bonded SiC, B which produces helium and BeO which migrates to grain boundaries. Also, the data of Thorne et al. [6], and Blackstone and Voice [8] on crusilite are excluded, because of the low initial density (about 70% of theoretical). When all these data are excluded, the remaining measurements shows more clearly a linear dependence of the saturation swelling on irradiation temperature.

(2) Balarin's model attributes swelling to single point defects and his analysis gives an effective mobility of migrating defects in the range 0.01–0.03 eV. Since he analyzed a limited temperature range (200–500°C), the temperature dependence, which is theoretically exponential, appears to be linear. However, if the same model is extended to higher temperatures, it would not reproduce the linear temperature dependence obtained from the previous data analysis. Moreover, the effective migration energies deduced from his analysis are well below our recent estimates using MD computer simulations.

(3) The simple phenomenological model presented here considers a sharp decrease in the concentration of interstitial loops with temperature and an increase in their average size. The net result is shown to give a linear dependence of the saturated value of volumetric swelling with temperature, in good agreement with valid experimental data over a wide range of temperatures (100–1000°C).

(4) The current model also shows agreement with average loop size, measured by Price [9]. Below approximately 700°C, the average size of interstitial loops is small, indicating that very few defects exist in each surviving cluster. In this range, macroscopic volumetric swelling measurements agree well with lattice dilatation measurements. However, at higher temperatures, lattice dilatation measurements give consistently lower values, in agreement

with our model and indicating the strong contribution from larger defect clusters to macroscopic swelling.

Acknowledgements

The authors wish to acknowledge the reviewer's comments, particularly on the analysis of experimental data and Dr Sharafat for his help with the English translation of Balarin's work. Financial support by the Office of Fusion Energy, US DOE under grant DE-FG03-91ER54115 with UCLA is greatly acknowledged.

References

[1] W. Primak, L. Fuchs, P. Day, Phys. Rev. 103 (5) (1956) 1184.
[2] N. Pravfyuk, V. Nikolaenko, V. Karpuchin, V. Kuznetsov, Investigation of diamond and silicon carbide as indicators of irradiation conditions, in: Properties of Reactor Materials and the Effects of Radiation Damage Proceedings, 1962.
[3] H. Suzuki, T. Iseki, M. Ito, J. Nucl. Mater. 48 (1973) 247.
[4] J. Palentine, J. Nucl. Mater. 61 (1976) 243–253.
[5] R. Price, Nucl. Technol. 16 (1972) 536.
[6] R. Thorne, V. Howard, B. Hope, Proc. Br. Ceram. Soc. 7 (1967) 449.
[7] R. Price, J. Nucl. Mater. 33 (1969) 17.
[8] R. Blackstone, E. Voice, J. Nucl. Mater. 39 (1971) 319.
[9] R. Price, J. Nucl. Mater. 48 (1973) 47.
[10] R. Price, T. Gulden, J. Kaae, Properties of Silicon Carbide Relevant to Its Performance as a Coating for High Temperature Fuel Properties, GMD-8415, 1968.
[11] R. Stevens, Philos. Mag. 25 (1972) 523.
[12] R. Mathews, J. Nucl. Mater. 51 (1974) 203.
[13] L. Rovner, G. Hopkins, Nucl. Technol. 29 (1976) 274.
[14] G. Hopkins, R. Price, Nucl. Eng. Design Fusion 2 (1985) 111.
[15] T. Suzuki, T. Maruyama, T. Iseki, T. Mori, M. Ito, J. Nucl. Mater. 149 (1987) 334.
[16] K. Hojou, K. Izui, J. Nucl. Mater. 133&134 (1985) 709.
[17] H. Miyazaki, T. Suzuki, T. Yano, T. Iseki, J. Nucl. Sci. Technol. 29 (7) (1992) 656.
[18] T. Suzuki, T. Iseki, T. Mori, J. Evans, J. Nucl. Mater. 170 (1990) 113.
[19] J. Corelli et al., Neutron irradiation experiments: Effects of boron isotopes, in: Ceramic Materials for Fusion Reactors, AP-2515, EPRI, 1982.
[20] S. Harrison, J. Corelli, J. Nucl. Mater. 99 (1981) 203.
[21] J. Corelli, J. Hoole, J. Lazzaro, C. Lee, J. Am. Ceram. Soc. 66 (7) (1983) 529.
[22] S. Harrison, J. Corelli, J. Nucl. Mater. 122&123 (1984) 833.
[23] K. Hojou, K. Izui, J. Nucl. Mater. 160 (1988) 147.
[24] T. Yano, T. Suzuki, T. Maruyama, T. Iseki, J. Nucl. Mater. 155–157 (1988) 311.
[25] T. Suzuki, T. Yano, T. Maruyama, T. Iseki, T. Mori, J. Nucl. Mater. 165 (1989) 247.
[26] T. Yano, K. Sasaki, T. Marnyama, T. Iseki, M. Ito, S. Onose, Nucl. Technol. 93 (1991) 412.
[27] T. Suzuki, T. Yano, T. Iseki, T. Mori, J. Am. Ceram. Soc. 73 (8) (1990) 2435.
[28] T. Iseki, T. Yano, H. Miyazaki, J. Nucl. Mater. 191–194 (1992) 588.
[29] C. Wu, J. Bonal, B. Kryger, J. Nucl. Mater. 208 (1994) 1.
[30] R. Price, Nucl. Technol. 35 (1977) 320.
[31] M. Balarin, Phys. Status Solidi 11 (1965) K67.
[32] H. Huang, N. Ghoniem, J. Nucl. Mater. 215 (1994) 148.
[33] H. Huang, N. Ghoniem, J. Wong, M. Baskes, Model. Simulat. Mater. Sci. Eng. 3 (1995) 615.
[34] T. Yano, T. Iseki, Philos. Mag. A 62 (4) (1990) 421.
[35] K. Tolpygo, Sov. Phys. Solid State 2 (1960) 2367.
[36] S. Sharafat, C. Wong, E. Reis, Fusion Technol. 19 (1991) 901.
[37] K. Maeda, K. Suzuki, S. Fujita, M. Ichihara, S. Hyodo, Philos. Mag. A 57 (1988) 573.
[38] H. Huang, N. Ghoniem, J. Nucl. Mater. 199 (1993) 221.